

## Supporting information

### The disrupted intracellular redox balance with enhanced ROS- generation and sensitive-drug release for cancer therapy

Dongmiao Sang<sup>1</sup>, Xiaofeng Li<sup>2</sup>, Zhikun Xu<sup>3</sup>, Huiming Lin<sup>1\*</sup>, Changhong Guo<sup>2\*</sup> and  
Fengyu Qu<sup>1\*</sup>

*1. Key Laboratory of Photochemical Biomaterials and Energy Storage Materials and College of  
Chemistry and Chemical Engineering, Harbin Normal University, Harbin 150025, China*

*2. College of life sciences and technology, Harbin Normal University, Harbin 150025, China*

Tel (Fax): +86 0451 88060653

E-mail: qufengyu@hrbnu.edu.cn, linhuiming@hrbnu.edu.cn, kaku\_2008@163.com

## **Experimental section**

### **Materials**

Unless specified otherwise, all of the chemicals were analytical grade and used without further purification.  $\text{SbCl}_3$  was purchased from Macklin. Se powder, CTAB,  $\text{NaBH}_4$ , 3-(Triethoxysilyl)propyl Isocyanate,  $\text{CH}_2\text{Cl}_2$ ,  $\text{Na}_2\text{SO}_4$ , Tetrahydrofuran and Dichlorofluorescein diacetate (DCFH-DA) were purchased from Aladdin Co. Ltd. propidium iodide (PI) were purchased from Alfa Aesar Co. Ltd. Isopropanol (IPA) was obtained from Sinopharm Chemical Reagent Co. Ltd. Calcein acetoxymethyl ester (calcein AM) was supplied by KeyGEN BioTCH. 3-(4,5-dimethyl-2-thiazolyl)-2,5-diphenyl-2-Htetrazolium bromide (MTT) was from Sigma Aldrich.

### **Characterization**

Transmission electron microscopy (TEM) images of samples were tested by Hitachi H-8100 at an accelerating voltage of 20 kV. Powder X-ray patterns (XRD) were tested on Rigaku Ultima IV diffractometer with Cu Ka radiation (40 kV, 20 mA). UV-Vis spectra were recorded on SHIMADZU UV2550 spectrophotometer. X-ray photoelectron spectroscopy (XPS) was detected with VG ESCALAB 220I-XL. The fluorescence spectra were surveyed by HORIBA FL-3. Zeta potential was carried out on a ZetaPALS Analyzer. Electron spin resonance (ESR) spectra were recorded on Burker A200 spectrometer with a modulation frequency of 100 kHz.

### **Synthesis of $\text{Sb}_2\text{Se}_3$ nanorods**

0.015 mol of selenium powder and 0.02 mol of  $\text{NaBH}_4$  were dissolved in 40 mL of ethanol, and then 0.01 mol of  $\text{SbCl}_3$  and 1 g of CTAB were added. After stirring for 30 min, the dispersion was put into Teflon-lined autoclave, and heated at 130 °C for 48 h. The obtained black product was washed with water and ethanol alternately for three times and dried at 60 °C.

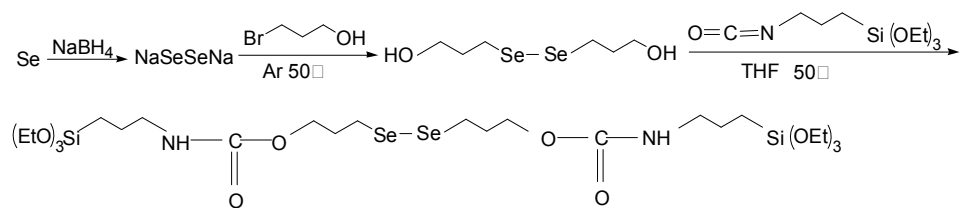
### **Synthesis of hollow $\text{Sb}_2\text{Se}_3@m\text{SiO}_2$ (SM) nanorods**

5.0 mg of  $\text{Sb}_2\text{Se}_3$  nanorods and 0.15 g of CTAB were dispersed in 10 mL of water (pH 9), stirred vigorously for 1 h. After that, 200  $\mu\text{L}$  of 20% TEOS in ethanol was injected twice at 30 min. The reaction mixture was stirred vigorously for 2.5 h. The  $\text{Sb}_2\text{Se}_3@m\text{SiO}_2$  was centrifuged and washed with ethanol. In order to remove the surfactant CTAB, 0.2 g of ammonium nitrate was dissolved in 50 mL of ethanol, and then  $\text{Sb}_2\text{Se}_3@m\text{SiO}_2$  was added and refluxed at 60 °C for 12 h. The product was centrifuged and collected.

### **Synthetic diselenide linker (-Se-Se- linker)**

We added 0.497 g of selenium powder into 25 mL of ice water with 0.5 g of  $\text{NaBH}_4$ . After 15 min, the solution was put into a steam bath to fully react to form  $\text{Na}_2\text{Se}_2$ . The generated  $\text{Na}_2\text{Se}_2$  solution was transferred into a 100 mL flask, sealed with a rubber plug and filled with argon, and then 20 mL of anhydrous THF solution with 12.6 mmol of 3-bromo-1-propanol was added into the above system. After reaction at 50 °C for 6 h, the solution was extracted three times with 20 mL of  $\text{CH}_2\text{Cl}_2$  and the obtained solution was dried with anhydrous  $\text{Na}_2\text{SO}_4$  overnight. After filtration,  $\text{CH}_2\text{Cl}_2$  solution containing HO-Se-Se-OH was obtained.

The  $\text{CH}_2\text{Cl}_2$  solution containing 1.35 mmol HO-Se-Se-OH was added into 5 mL of anhydrous THF was injected with Ar flowing. And then, added 2 mL of anhydrous THF with 1.49 mmol of 3-(triethoxy silyl) propyl isocyanate, and reacted in a 50 °C oil bath for 12 h to obtain a yellow transparent product  $3(\text{EtO})\text{Si-Se-Se-Si}(\text{OEt})_3$ .



### Drug loading ( $\text{Sb}_2\text{Se}_3@m\text{SiO}_2\text{-DOX-Se-Se}$ , SMDS) and release

70 mg of  $\text{Sb}_2\text{Se}_3@m\text{SiO}_2$  and 1.5 mg of DOX were added to the PBS solution (8 mL) and stirred at room temperature for 12 h. Next, 5, 10 and 15  $\mu\text{L}$  of -Se-Se-linker solution was dropped into the mixed solution. The obtained solid was named as SMDS-1, SMDS-2, SMDS-3, respectively). The amount of loaded DOX was estimated by UV-Vis spectroscopy at 480 nm.

$$\text{Encapsulation efficiency (wt.\%)} = \frac{m_{(\text{original Dox})} - m_{(\text{residual Dox})}}{m_{(\text{original Dox})}} \times 100\%$$

Where  $m_{(\text{original Dox})}$  and  $m_{(\text{residual Dox})}$  reveals the mass of the original and residual Dox in the supernatant, respectively. The packaging efficiency of DOX is 80.3 %

30 mg of SMD were dispersed in the 30 mL of PBS (pH = 6.5) with and without NIR irradiation. The corresponding supernatant was centrifuged at intervals, and the absorbance of DOX was measured by UV-Vis. The content of released Dox was corresponding to the standard curve.

### Synthesis of $\text{Sb}_2\text{Se}_3@m\text{SiO}_2\text{-DOX-Se-Se-PEG}$ (SMDSP)

(0.7 mmol) PEG was dissolved 5 ml of anhydrous THF in a 20 mL three neck flask, sealed with a rubber plug, injecting Ar for 20 min, and then added 2 ml of anhydrous THF containing 1.49 mmol of propyl triethoxysilane isocyanate with the syringe. The whole process was carried out under Ar at 50 °C for 12 h. Finally,  $\text{NH}_2\text{-PEG+O=N=C-Si}(\text{OEt})_3$  can be obtained.

Put the drug loaded material into a brown bottle, added the prepared  $3(\text{Eto})\text{Si-Se-Se-Si}(\text{Eto})_3$  (300  $\mu\text{L}$ ), stirred at room temperature for 2 h, then added  $\text{NH}_2\text{-PEG+O=N=C-Si}(\text{OEt})_3$  (300  $\mu\text{L}$ ) for another 6 h. The product was collected, washed and dry to obtain SMDSP.

#### **Photothermal performance test**

1 mL of sample dispersion was placed in a cuvette with different concentrations (0, 25, 50, 100, 200  $\mu\text{g mL}^{-1}$ ) and illuminated (808-nm laser) for 10 min with different power densities. And the temperature was measured by FLIR infrared thermal imager E8.

#### **Photodynamic performance test**

100  $\mu\text{L}$  of DCFH-DA (6  $\text{mg mL}^{-1}$ ) was added into 1 mL of sample dispersion (100  $\mu\text{g mL}^{-1}$ ) and irradiated at 808 nm for different times. The supernatant was collected by centrifugation and detected by fluorescence.

ESR (electron spin resonance) can confirm the specific species of ROS. Here, DMPO and TMEP were used as spin trapping agents. During the experiment, the mixture solution containing the prepared sample and trapping agent was transferred to ESR tube and irradiated with 808 nm laser for 4 min.

#### **Cell culture**

Two kinds of cells, HepG2 (hepatoma cell line) and BEAS-2B cells (Epithelial cells of bronchus), were selected in this study. All cells were cultured in Dulbecco's Modified Eagle's Medium (DMEM, HyClone) with 10% (v/v) fetal bovine serum

(FBS, Tianhang Bioreagent Co., Zhejiang) and penicillin ( $100 \text{ U mL}^{-1}$ ) and streptomycin ( $100 \text{ mg mL}^{-1}$ ) in a humid atmosphere of 5%  $\text{CO}_2$  at  $37 \text{ }^\circ\text{C}$ .

### **MTT assay**

HepG2 cells and BEAS-2B cells were seeded in 96 well plates with 10000 cells per well and cultured overnight to make sure the attachment. And then, these cells were incubated with different samples with varying concentrations. After 12 h of culture, the medium was extracted and washed gently with PBS to remove the noninternalized material. Later, the cells were irradiated with 808-nm NIR for 20 min. After that,  $20 \text{ }\mu\text{L}$  of MTT solution ( $5 \text{ mg mL}^{-1}$ ) was added and these media was sucked out after 4 h incubation. Finally,  $150 \text{ }\mu\text{L}$  of DMSO was put in and the absorbance was monitored using a microplate reader (WD-2102A) at the wavelength of 492 nm.

### **Intracellular ROS**

The production of reactive oxygen species in cells can also be monitored by DCFH-DA. All cells were seeded on 6-well plate for 24 h, and then SMP and SMSP ( $60 \text{ }\mu\text{g mL}^{-1}$ ,  $1 \text{ mL}$ ) were co-cultured for 12 h. After the washing for 3 times with PBS,  $10 \text{ }\mu\text{mol L}^{-1}$  DCFH-DA was added. 1 h later, cells were further washed 3 times with PBS, and irradiated with 808-nm light for 10 min, and finally imaged by Leica DFC450 C Microsystems Ltd.

### **Fluorescence imaging**

In order to observe the uptake and intracellular drug release of SMDSP in HepG2 cells, which were co-cultured with SMDSP ( $1 \text{ mL}$ ,  $100 \text{ g mL}^{-1}$ ) for 0.5, 1,

3h and 3h with irradiation. Then the nuclei were stained with DAPI (4',6-diamidino-2-phenylindole) and washed with PBS three times. Finally, imaging by using Leica DFC450 C Microsystems Ltd..

HepG2 cells were cultured in a single orifice plate for 24 h, then 2 mL of SMDSP (0, 50, 100  $\mu\text{g mL}^{-1}$ ) was added and cultured for 12 h to make sure the uptake. The single orifice plate was irradiated with 808-nm of different power density for 20 min, and then placed in the incubator for 4 h. Then, sucked out the media and washed gently with PBS for three times. AM was added to culture for 30 min, then PI was added to culture for 10 min. Finally, the image was imaged under Leica DFC450 C Microsystems Ltd..

### ***In vitro* and *vivo* CT imaging**

In order to demonstrate the CT imaging ability, SMP was tested *in vitro* and *in vivo*. Dispersing different concentration of SMP nanorods in aqueous solution (0, 0.9375, 1.875, 3.75, 7.5, 15.0 and 30.0  $\text{mg mL}^{-1}$ ) were placed into centrifuge tubes to obtain the CT images *in vitro*. For the *in vivo* CT imaging of SMP nanorods, the tumor-bearing mice were anesthetized and then were injected with 100  $\mu\text{L}$  dispersions of SMP (1  $\text{mg mL}^{-1}$ ). Before and after injection, the axial and coronal positions of mice were imaged. Both the *in vitro* and *in vivo* CT imaging were acquired on a Philips 64-slice CT imaging system.

### ***In vivo* toxicity**

We selected female Kunming mice with a weight of 30 g as the experimental object. The H22 cells were injected into the armpit of mice and formed a solid tumor

about 350 mm<sup>3</sup> in volume. The mice were divided into four groups randomly: saline, SMDSP, NIR and SMDSP + NIR group. For SMDSP and SMDSP + NIR group, the sample suspension (250 µg mL<sup>-1</sup>, 100 µL) was injected intravenously. And the NIR illumination was performed under 1 W cm<sup>-2</sup> for 10 min. Real time recording of tumor temperature was carried out with thermal imager during irradiation. All the treatments were carried out every 4 days for 14 days. The body weights and the tumor size were measured and recorded every two days.

### **Histological examination**

After 14 days of treatment, four groups of mice with different treatments were taken out of the heart, liver, spleen, lung, kidney and tumors. Then the excised tissues were dehydrated using buffered formalin, various concentrations of ethanol, and xylene. Subsequently, the dehydrated tissues were encased by liquid paraffin, which sliced and stained with hematoxylin and eosin (H&E). After staining, the slices were observed by optical microscope (Leica DFC450 C).

### **Haematological Analysis**

After the treatment for 14 day, the blood (20 µL) of mice were collected and measured by automatic blood analyzer (HF-3800).



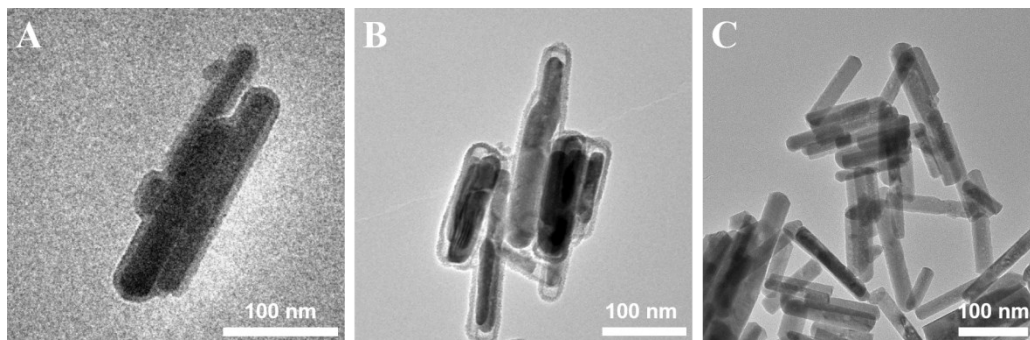


**Fig. S1** TEM images of  $\text{Sb}_2\text{Se}_3@m\text{SiO}_2$  nanorods (A) without removing the surfactant CTAB. (B) The movement of surfactant CTAB once. (C) The movement of surfactant CTAB twice.

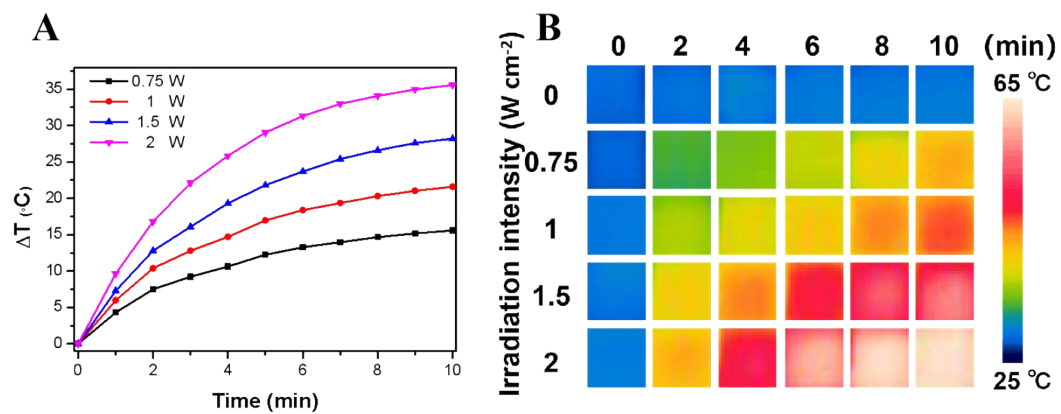


**Fig. S2** (A) Photothermal heating curves of SM nanorods ( $100 \mu\text{g mL}^{-1}$ ) and (B) Infrared thermal images of aqueous dispersions under 808 nm irradiation with different power densities.

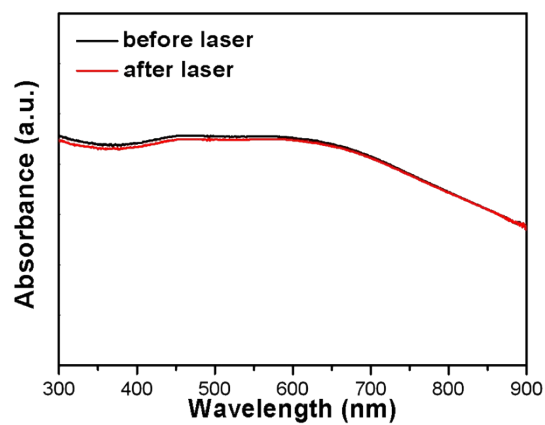


**Fig. S3** The UV-Vis absorption spectra of SM nanorods before and after 4 times of illumination on-off,

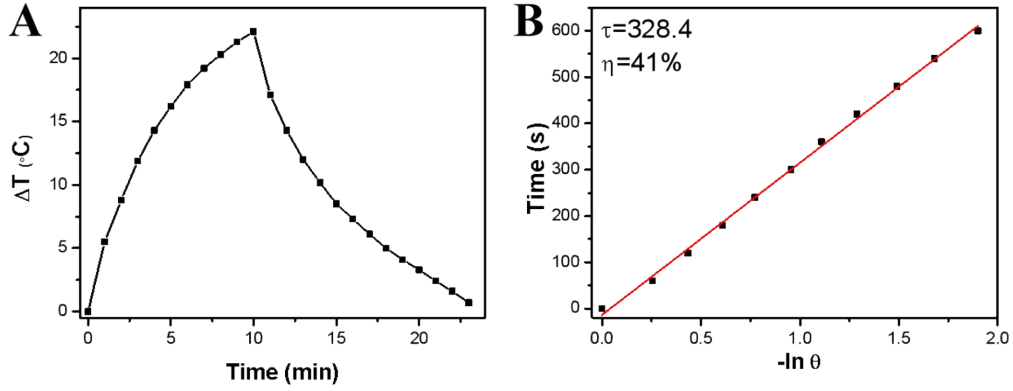


**Fig. S4** (A) Temperature evolution of the dispersion of these SM nanorods during heating (laser on) and cooling (laser off). (B) Thermal equilibrium time constants of the system determined by fitting the time data versus the negative natural logarithm of the driving force temperature from the cooling period.

The photothermal properties of materials are embodied by the photothermal conversion efficiency which is calculated by the following formula (1):

$$\eta = \frac{hA(T_{\max} - T_a) - Q_0}{I(1 - 10^{-A\lambda})} \quad (1)$$

$T_{\max}$  represents the highest temperature of the system, and  $T_a$  represents the ambient temperature.  $I$  is the power of laser, 750 mW is used in this paper.  $A\lambda$  is the absorption of the SM suspension at 808 nm in Fig. 2A.  $Q_0$  is the energy absorbed by pure water under 808-nm laser irradiation, and  $h$  and  $A$  is the heat transfer coefficient and the area of light point, respectively. Finally,  $hA$  needs to be calculated by the following formula (2) to (4).

$$\tau = \frac{m_D C_D}{hA} \quad (2)$$

$$\theta = \frac{T - T_a}{T_{\max} - T_a} \quad (3)$$

$$\ln \theta = -\frac{t}{\tau} \quad (4)$$

$T$  is the systematic temperature at random time during the cooling process.  $\tau$  is the system time constant (328.4 s), as shown in Fig. S4B.  $C_D$  and  $m_D$  represent the specific heat capacity (4.2 J/g·°C) and mass (1.0 g) of water respectively.

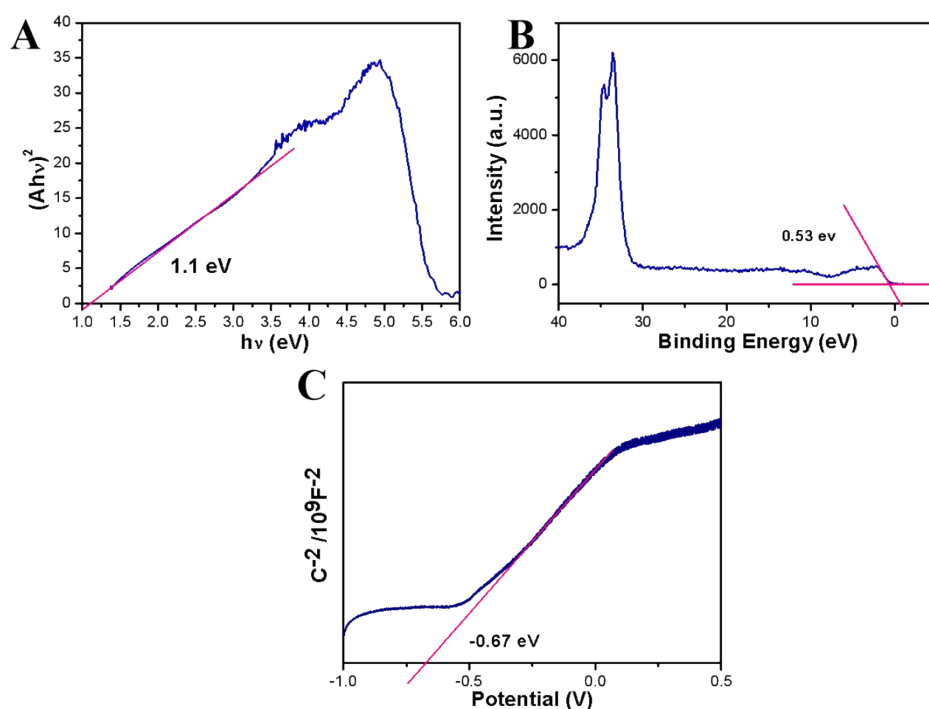


**Fig. S5** (A) The  $(Ah\nu)^2$  versus  $h\nu$  curve. (B) valence-band XPS spectrum and (C) Mott-Schottky (MS) curve of  $Sb_2Se_3$ .

We calculate  $E_g$  by the following formula:

$$\alpha h\nu = A (h\nu - E_g)^{n/2}$$

The  $n$  of direct and indirect semiconductors are 1 and 4, respectively. By consulting the literature that  $Sb_2Se_3$  is a indirect semiconductor and making a tangent line with the x-axis, the band gap of  $Sb_2Se_3 = 1.1$  eV in Fig. S5A.

As shown in Fig. S5B, the VB value of  $Sb_2Se_3$  is 0.53 eV (vs. Fermi level) from VB XPS spectrum. We measured the Fermi level of  $Sb_2Se_3$  through the electrochemical workstation. In fact, the Mott-Shottky curve measurements were taken to reveal the flat band potential ( $E_{fb}$ ) of the material, which is numerically

equal to the Fermi level. The flat band potential measured in Fig. S5C is -0.67 eV (vs. Ag/AgCl at pH=6.8), according to the following equations:

$$E_{(NHE)} = E_{(Ag/AgCl)} + 0.197$$

$$E_{(RHE)} = E_{(NHE)} + 0.0591pH$$

The value was calculated to be -0.07V of synthesized  $Sb_2Se_3$ . Additionally, the epitaxial tangents of the Mott-Schottky plots uniformly show positive slope, indicating the samples are n-type semiconductors. It is known that the flat potential is equal to the Fermi level ( $E_f$ ) for n-type semiconductors, whereby the  $E_f$  of  $Sb_2Se_3$  is -0.07 eV.

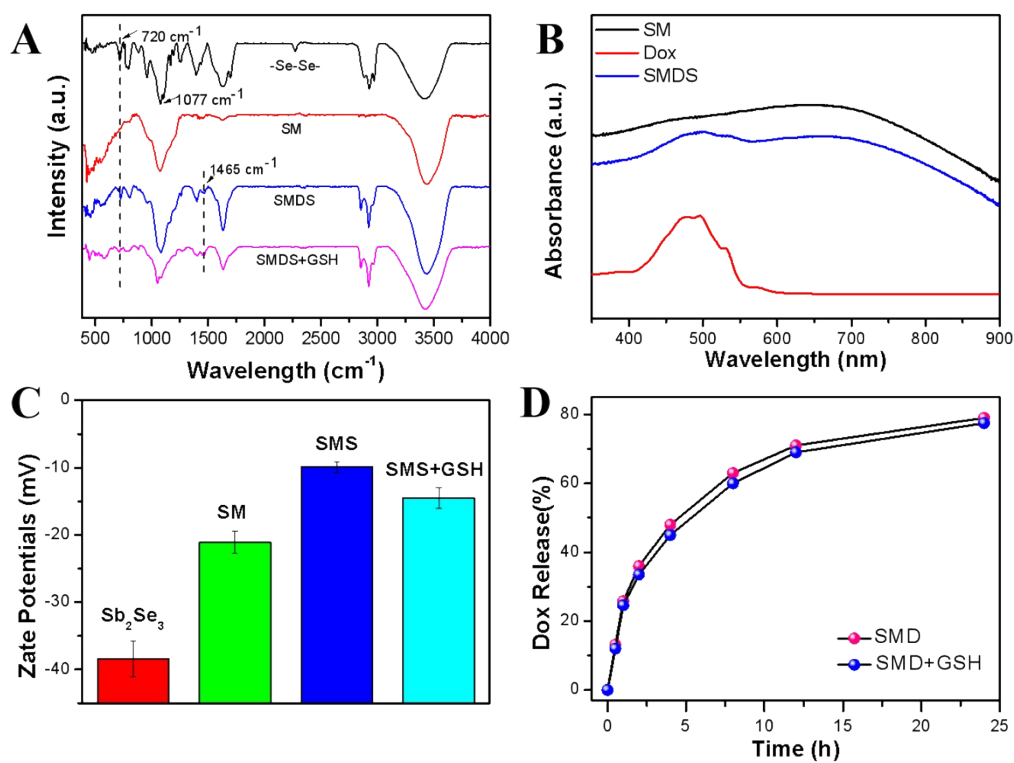


**Fig. S6** (A) FTIR spectra of -Se-Se- linker, SM, SMDS and SMDS+GSH. (B) UV-Vis absorption spectra for SM, Dox, and SMDS. (C) Zeta potentials for  $\text{Sb}_2\text{Se}_3$ , SM, SMS, and SMS+GSH and (D) Dox release of SMD and SMD+GSH in PBS (pH 6.5).



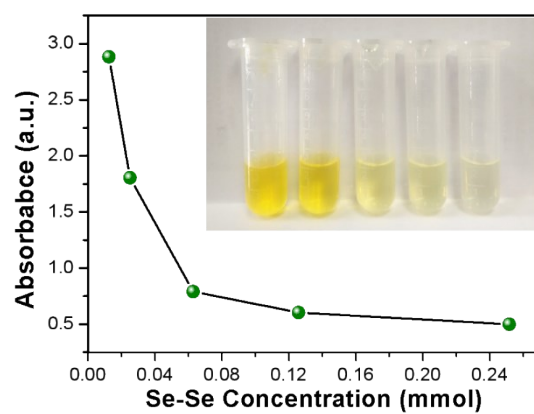


**Fig. S7** GSH depletion under the different concentrations of Se-Se linker.

	T1 (0-12h)	T2 (12-48h)
SMDS-1+GSH	19.92	6.18
SMDS-2+GSH	17.21	5.99
SMDS-3+GSH	14.98	3.51
SMDS-1	2.36	
SMDS-2	1.92	
SMDS-3	1.60	

**Table S1** The summary of drug diffusion coefficient for SMDS with/without GSH.

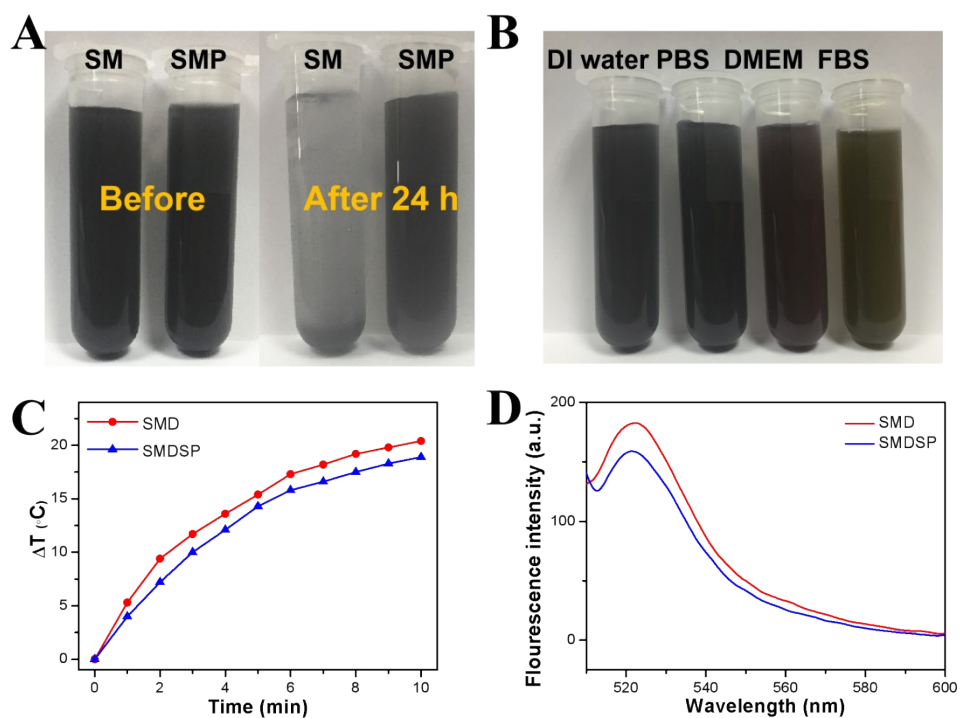


**Fig. S8** (A) Dispersion of SM nanorods before and after PEG modification. (B) Dispersion of SMP nanorods in different solutions. (C) Photothermal curves and (D) Fluorescence spectra of DCFH-DA incubated with SMD and SMDSP nanorods ( $100 \mu\text{g mL}^{-1}$ ) under different irradiation time ( $808 \text{ nm}$ ,  $1 \text{ W cm}^{-2}$ ).

It is known that the PEGylation aims at the improved dispersion stability of nanocomposite. However, the photothermal and photodynamic performances of SMDSP decreased slightly due to the inactive PEG.

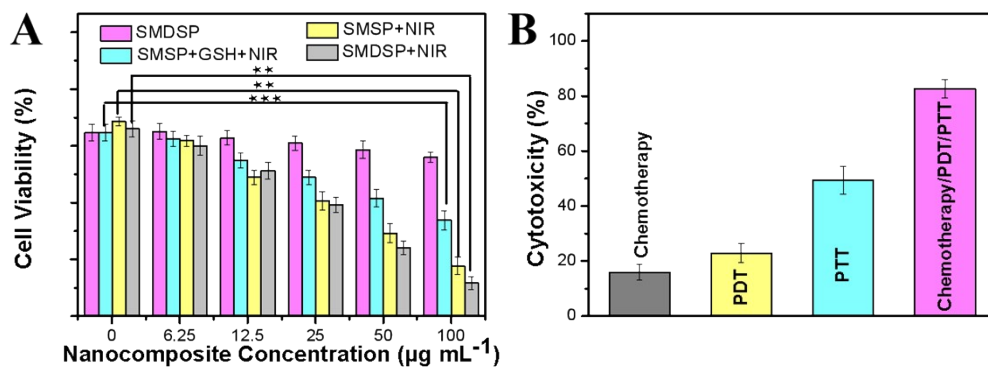


**Fig. S9** (A) Cell Viability of HepG2 incubated with the SMSP and SMDSP nanorods at different concentrations, (B) Cytotoxicity of chemotherapy, PDT, PTT and synergistic therapy for HepG2 cells with sample concentration  $100 \mu\text{g mL}^{-1}$ .